2006

Vomeronasal Sensory Neurons from Sternotherus Odoratus (Stinkpot/Musk Turtle) Respond to Chemosignals via the Phospholipase C System

Jessica H. Brann
Loyola University Chicago, jbrann@luc.edu

Debra A. Fadool

Published in final edited form as:
J Exp Biol. 2006 May ; 209(Pt 10): 1914–1927. doi:10.1242/jeb.02206.

Vomeronasal sensory neurons from *Sternotherus odoratus* (stinkpot/musk turtle) respond to chemosignals *via* the phospholipase C system

Jessica H. Brann[1,*] and **Debra A. Fadool**[1,2,†]

[1]The Florida State University, Department of Biological Science, Program in Neuroscience, Biomedical Research Facility, Tallahassee, FL 32306, USA

[2]The Florida State University, Department of Biological Science, Program in Molecular Biophysics, Biomedical Research Facility, Tallahassee, FL 32306, USA

Summary

The mammalian signal transduction apparatus utilized by vomeronasal sensory neurons (VSNs) in the vomeronasal organ (VNO) has been richly explored, while that of reptiles, and in particular, the stinkpot or musk turtle *Sternotherus odoratus*, is less understood. Given that the turtle's well-known reproductive and mating behaviors are governed by chemical communication, 247 patch-clamp recordings were made from male and female *S. odoratus* VSNs to study the chemosignal-activated properties as well as the second-messenger system underlying the receptor potential. Of the total neurons tested, 88 (35%) were responsive to at least one of five complex natural chemicals, some of which demonstrated a degree of sexual dimorphism in response selectivity. Most notably, male VSNs responded to male urine with solely outward currents. Ruthenium Red, an IP_3 receptor (IP_3R) antagonist, failed to block chemosignal-activated currents, while the phospholipase C (PLC) inhibitor, U73122, abolished the chemosignal-activated current within 2 min, implicating the PLC system in the generation of a receptor potential in the VNO of musk turtles. Dialysis of several second messengers or their analogues failed to elicit currents in the whole-cell patch-clamp configuration, negating a direct gating of the transduction channel by cyclic adenosine monophosphate (cAMP), inositol 1,4,5-trisphosphate (IP_3), arachidonic acid (AA), or diacylglycerol (DAG). Reversal potential analysis of chemosignal-evoked currents demonstrated that inward currents reversed at −5.7 ±7.8 mV (mean ± s.e.m.; *N*=10), while outward currents reversed at −28.2±2.4 mV (*N*=30). Measurements of conductance changes associated with outward currents indicated that the outward current represents a reduction of a steady state inward current by the closure of an ion channel when the VSN is exposed to a chemical stimulus such as male urine. Chemosignal-activated currents were significantly reduced when a peptide mimicking a domain on canonical transient receptor potential 2 (TRPC2), to which type 3 IP_3 receptor (IP_3R3) binds, was included in the recording pipette. Collectively these data suggest that there are multiple transduction cascades operational in the VSNs of *S. odoratus*, one of which may be mediated by a non-selective cation conductance that is not gated by IP_3 but may be modulated by the interaction of its receptor with the TRPC2 channel.

Keywords

olfaction; VNO; transduction; PLC; TRPC2; inositol 1,4,5-trisphosphate receptor (IP_3R); musk turtle; *Sternotherus odoratus*

†Author for correspondence (e-mail: dfadool@bio.fsu.edu).
*Present address: 920 Fairchild Center, MC 2439, Department of Biological Sciences, Columbia University, New York, NY 10027, USA

Introduction

The accessory olfactory system (AOS) has been well established as a primary detector for odor information concerning social organization and reproductive status (Halpern and Martínez-Marcos, 2003). In addition, in reptilian species such as the turtle, lizard and garter snake, the AOS also serves to detect prey items (Wang et al., 1997; Fadool et al., 2001; Vitt et al., 2003). The best-studied peripheral sensory organ for the AOS is the vomeronasal organ (VNO). Sexual dimorphism in the reptilian and amphibian VNO is found at both the level of gross anatomy (Dawley, 1998) and the single sensory neuron (Fadool et al., 2001). There are sexually distinct differences in vomeronasal sensory neuron (VSN) soma diameter as well as in the composition and kinetics of voltage-activated conductances (Fadool et al., 2001).

In terrestrial vertebrates, the VNO is a compartment of the olfactory system that is separate and distinct from the main olfactory system (MOS). In reptiles, it is larger than the main olfactory epithelium (MOE), the sensory organ for the MOS (Ernst et al., 1994; Murphy et al., 2001; Labra et al., 2005). In most animal classes, the VNO is thought to mediate primarily pheromonal signals, but not exclusively (Baxi et al., 2006). Pheromones [originally described by Karlson and Lüscher (Karlson and Lüscher, 1959)] are substances that are secreted to the external environment by an individual and received by a second individual of the same species, in which they release a specific reaction, for example, a definite behavior or a developmental process (Rodriguez et al., 2002). While the VNO is responsive to pheromones, it also detects a variety of chemosignals that may not fit within the classical definition of a pheromone. Often, the VNO is considered a detector of nonvolatile odorants, but this assertion is incorrect, since the VNO detects volatile odorants as well (O'Connell and Meredith, 1984; Meredith, 1991; Meredith, 2001; Halpern and Martínez-Marcos, 2003; Trinh and Storm, 2003; Leinders-Zufall et al., 2004). In addition, the MOE is known to respond to some pheromones (Restrepo et al., 2004). Hence we will use the term 'chemosignal' to incorporate any chemical received by the VNO and potentially able to elicit an electrical signal encoded by this organ for chemical communication.

Although a limited amount of published molecular chemoreceptor information is available for reptiles (i.e. Vogt et al., 2002), it is generally believed that the initial VNO transduction event is governed by the binding of chemosignals to G-protein coupled receptors (GPCRs), as well described for rodents (Dulac and Axel, 1995; Herrada and Dulac, 1997; Matsunami and Buck, 1997; Ryba and Tirindelli, 1997; Pantages and Dulac, 2000). Although the nucleotide sequence and expression patterns of these receptors have not yet been published for the reptilian VNO, we do know that in the common musk/stinkpot turtle *Sternotherus odoratus* they must be coupled to the downstream G-protein $G_{\alpha i}$, which has restricted expression in the microvilli of the turtle VSNs, is expressed at greater levels in male *versus* female turtle VNO, and is developmentally increased in the VNO coincident with reproductive maturity of the turtles (Murphy et al., 2001). More is known for the downstream signaling cascade found in this species, in which there appears to be continuity with that known for rodents. Rodent VSNs utilize phospholipase C (PLC) signaling (Runnenburger et al., 2002) to cleave phosphatidyl-inositol *bis*-phosphate (PIP_2) into diacylglycerol (DAG) and inositol 1,4,5-trisphosphate (IP_3) second messengers (Berridge and Irvine, 1984). DAG or one of its derivatives, arachidonic acid (AA), may activate the ion channel responsible for carrying the chemosignal-activated current, the canonical transient receptor potential channel, TRPC2 (Spehr et al., 2002; Lucas et al., 2003). This channel is a six-transmembrane domain nonselective cation channel and is a member of the TRP ion channel superfamily (Minke and Cook, 2002). TRPC2 is expressed in the microvilli of rats, mice and turtles (Liman et al., 1999; Murphy et al., 2001; Leypold et al., 2002; Stowers et al., 2002). In both rodents and turtles, TRPC2 shows a developmental pattern of expression, with an increased expression correlated to sexual maturity (Murphy et al., 2001). TRPC2 and the type III inositol 1,4,5-trisphospate receptor (IP_3R3)

demonstrate co-localization in VSN microvilli and can be co-immunoprecipitated from rodent VNO (Brann et al., 2002), but the functional relevance of this protein–protein interaction is yet unknown.

Several questions remain unanswered, therefore, when discussing transduction in the VNO of *S. odoratus* and downstream vertebrate VNO transduction in general. First, it is not clear whether PLC signaling is important to the generation of a receptor potential in the turtle VNO. Second, it is unknown if, and how, TRPC2 is activated in the turtle. Third, TRPC2 in mouse VSNs was shown to be activated by an analogue of diacylglycerol (DAG), independently of IP_3 (Lucas et al., 2003), therefore it is unknown if a TRPC2/IP_3R3 complex is required for the final transduction event, or simply provides a form of modulation of the transduction current. Fourth, DAG (and its derivatives) has now been shown to activate TRPC3 and TRPC6 (Chyb et al., 1999; Hofmann et al., 1999; Clapham et al., 2001; Venkatachalam et al., 2001; Albert and Large, 2003; Pocock et al., 2004), and may also have a role in the VNO (Spehr et al., 2002; Lucas et al., 2003). The dialysis of a natural DAG analogue (called SAG) into rodent VSNs, however, did not elicit a current with chemosignal-like kinetics. Nonetheless, the effectiveness of SAG as an activator of the cation channel was severely diminished in TRPC2-null mice, suggesting that TRPC2 is the channel activated by SAG (Lucas et al., 2003). DAG has been reported to not activate TRPC1, TRPC4 or TRPC5 (Hofmann et al., 1999; Venkatachalam et al., 2003). Together, these studies demonstrate a putative direct role of DAG in gating TRPC2, but do not address possible modulation, amplification or regulation of the primary cationic conductance by IP_3Rs mediated by the protein–protein interaction between TRPC2 and IP_3R3.

Here, we explore currents elicited with several natural chemosignals, including urine, a reproductive musk and a prey item. The use of the PLC system in the transduction of chemosignal information is examined pharmacologically, and reversal potential analysis is used to demonstrate the presence of two separate ionic conductances found in the musk turtle VNO. Finally, the role of the signaling complex between TRPC2 and IP_3R3 in the turtle is examined by disruption of the complex with a peptide inhibitor.

Materials and methods

Animal collection, care, and maintenance

Sternotherus odoratus Latreille (stinkpot or common musk turtle) were hand-caught during the reproductive season (April to September) at Indian Pines (Opelika, AL, USA) or Lake Jackson (Tallahassee, FL, USA) with permission from the State of Alabama Department of Conservation and the State of Florida Fish and Wildlife Conservation Commission. Turtles were housed for short periods, usually 1–2 months, in 10 gallon (38 l) aquaria with rocks for basking, maintained on a 15 h:9 h light:dark cycle and fed a standard diet of catfish pellets (Florida Farm and Feed, Tallahassee, FL, USA). Turtles used in the described experiments were adults (Ernst et al., 1994; Fadool et al., 2001). Mass and plastron length were noted on the day of capture as well as on the day of experimental use. The plastron, or ventral shell, of a turtle is often used to measure growth or size of the animal, given the more variable curvature of the dorsal carapace (Ernst et al., 1994). All procedures were performed in accordance with The Florida State University Animal Care and Use Committee.

Solutions

Ca^{2+}-free Ringer contained (in mmol l^{-1}): 116 NaCl, 4 KCl, 1 $MgCl_2$, 15 glucose, 10 Hepes, 10 EGTA, pH 7.4. Ringer contained (in mmol l^{-1}): 116 NaCl, 4 KCl, 1 $CaCl_2$, 1 $MgCl_2$, 15 glucose, 10 Hepes, 5 sodium pyruvate, pH 7.4. Pipette solution contained (in mmol l^{-1}): 100 KCl, 20 NaCl, 10 Hepes, 2 $MgCl_2$, 1.1 EGTA, 0.8 $CaCl_2$, 2.5 ATP, 0.5 GTP, pH 7.4. Phosphate-

buffered saline (PBS) contained (in mmol l^{-1}): 137 NaCl, 2.7 KCl, 10 Na_2HPO_4, 2 KH_2PO_4, pH 7.4. All chemicals were obtained from either Sigma Chemical Company (St Louis, MO, USA) or Fisher Scientific (Fairlawn, NJ, USA).

Electrophysiology

Turtles were killed by administering a lethal intraperitoneal dose of sodium pentabarbitol (Butler Company, Columbus, OH, USA), followed by decapitation. The VNO was quickly dissected, grossly cut into quarters, and incubated in *L*-cysteine-activated papain (Worthington Biochemical Corp., Lakewood, NJ, USA) in Ca^{2+}-free Ringer for 15–18 min while gently rotated at 30 r.p.m. (Orbital Shaker, Model 3520, Lab-Line Instruments, Melrose Park, IL, USA) at room temperature (RT). Following enzymatic treatment, quarters could be held at 4° C for up to 8 h prior to physical dissociation. Sensory neurons were physically dissociated by trituration using a size-graded series of fire-polished siliconized Pasteur pipettes and were then plated on to 0.01% poly-D-lysine hydrobromide (Sigma) and 0.1% laminin (BD Biosciences, San Jose, CA, USA) coated Corning #25000 dishes (Fisher) (Leinders-Zufall et al., 1997).

Acutely isolated vomeronasal sensory neurons (VSNs) were viewed at 40× magnification (Axiovert 135, Carl Zeiss, Thornwood, NY, USA) with Hoffman modulation contrast optics for patch-clamp recording (Hamill et al., 1981). Patch pipettes were fabricated from Jencons borosilicate glass (catalog number M15/10; Jencons Limited, Bedfordshire, UK), fire-polished to approximately 1 μm (bubble number 5.0) (Mittman et al., 1987) and coated near the tip with beeswax to reduce the pipette capacitance. Pipette resistances were between 7 and 10 MΩ, which produced high-resistance seals (between 8 and 14 GΩ) by applying gentle suction to the lumen of the pipette upon contact with the cell. In all experiments, cells were voltage-clamped at a holding potential (V_h) of −60 mV, unless specified otherwise. Voltage- and chemically activated currents were recorded in the whole-cell configuration using an integrating patch-clamp amplifier (Axopatch 200B, Axon Instruments, Union City, CA, USA). The analog output was filtered at 5 kHz and digitally sampled every 0.5–4 ms. Data acquisition, storage and analysis of the digitized recordings were carried out using pClamp8.0 software (Axon Instruments) in conjunction with Origin 4.1 (Microcal Software, Inc., Northampton, MA, USA), SigmaPlot 8.0 and SigmaStat 3.0 (Systat Software, Point Richmond, CA, USA). Statistical tests are as noted, with statistical significance in all tests defined at the 95% confidence interval (Steel and Torrie, 1980).

Second messengers and pharmacological agents

Second messengers and non-permeant analogues were introduced *via* the pipette during whole-cell recording. To promote seal formation and initial controlled recording conditions, pipettes were tip-filled 1–2 mm with control patch solution and then back-filled with messenger or analogue; a method we have previously calibrated and applied (Fadool and Ache, 1992). Cyclic adenosine monophosphate (cAMP; 0.5 or 1 μmol l^{-1}; back-fill pipette; Sigma) and inositol 1,4,5-trisphosphate (IP_3; 1–100 μmol l^{-1}; back-fill pipette, Sigma) were made as a stock solution stored at −20°C and diluted in pipette solution daily. Arachidonic acid (AA; 10 μmol l^{-1}; back-fill pipette; Calbiochem, San Diego, CA, USA), a non-cell permeable polyunsaturated fatty acid (PUFA) derived from DAG by a DAG lipase or from phospholipids by phospholipase A_2 (Spehr et al., 2002), was prepared fresh daily in pipette solution. 1-Oleoyl-2-acetyl-*sn*-glycerol (OAG; 100 μmol l^{-1}; both bath application and back-fill pipette tested; Calbiochem) and 1-stearoyl-2-arachidonoyl-*sn*-glycerol (SAG; 100 μmol l^{-1}; back-fill pipette; Calbiochem), analogues of diacylglycerol (DAG), were reconstituted daily in DMSO (final concentration ≤0.1%). Ruthenium Red (RR), shown to inhibit IP_3-evoked currents (Fadool and Ache, 1992; Kashiwayanagi et al., 2000; Taniguchi et al., 2000), was freshly made daily in Ringer at a concentration of 1 mmol l^{-1} and filtered (25 mm diameter, 0.2 μm pore size, Whatman, Clifton, NJ, USA) to avoid occlusion of the multi-barrel pipette (bath

application; Sigma). U73122, an inhibitor of phospholipase C, was reconstituted in DMSO (final concentration ≤0.1%) and stored at −20°C as a stock solution (50 μmol l^{-1}; bath application; BioMol, Plymouth Meeting, PA, USA). A synthesized peptide (10 μmol l^{-1}) designed to target and interrupt the interaction domain between TRPC2 and IP_3R3 with the peptide sequence GSAGEGERVSYRLRVIKALVQRYIETARRE (905–934 mTRPC2) (Tang et al., 2001) was reconstituted in pipette solution and stored at −20°C until use (back-fill pipette; GeneMed Synthesis, Inc., South San Francisco, FL, USA). Based upon the mouse sequence for TRPC2 (GenBank accession no. AAD17196) (Vannier et al., 1999), we utilized web-based protein prediction software (called TMpred – Prediction of Transmembrane Regions and Orientation; http://www.ch.embnet.org/software/TMPRED_form.html,) to determine that the predicted binding would align with the intracellular C-terminal tail of the channel (Hofmann and Stoffel, 1993; Hirokawa et al., 1998).

Chemical stimulation

During the reproductive season (April–September), musk was harvested from *Sternotherus odoratus* once a month by gently milking the posterior reproductive musk gland. Musk samples obtained from a single animal ranged between 1–2 μl. Turtle urine was obtained *post mortem* by inserting a 27-gauge needle directly into the bladder. Catfish extract was prepared from a commercially available pellet (Florida Farm and Feed, Tallahassee, FL, USA). Pellets (2 g) were hydrated in 20 ml of high-quality water, ground by mortar and pestle, and then clarified by low-speed centrifugation for 5 min at room temperature. All samples were rapidly collected, placed on ice, and stored undiluted at −80°C until diluted in Ringer on the day of experimentation.

Chemosignals were spritzed (700 ms pulse) onto isolated VSNs using custom-fabricated seven-barrel glass micropipettes (1.2mm outer diameter, catalog no. 17-12-M; Frederick Haer, Bowdoinham, ME, USA) coupled to a pressurized valve system (Picospritzer, General Valve, Fairfield, NJ, USA). Dilution of the chemical between the multibarrelled pipette and the cell surface, an average distance of two cell diameters, was estimated to be approximately 9% on the basis of the calculated K^+ permeability method (Firestein and Werblin, 1989). Chemical concentrations are reported as the pipette concentration and are not corrected for this dilution. The pipette concentration of urine was 1:5 from full strength, between 1:100 and 1:300 for musk, and between 1:100 and 1:1000 for catfish extract. All dilutions were prepared daily in turtle Ringer, which served as the control vehicle in all conditions. If a neuron responded to the control, it was assumed to be a mechanical stretch-activated response, and no further use was made of the cell. The peak magnitude of a response was measured as the difference in current from the baseline prior to presentation of the chemical to the peak outward- or inward-evoked current within 500 ms of valve activation of the picospritzer. Zero current (no response) was defined as no observable deflection or a deflection that was less than four times the total peak-to-peak (range) noise level (membrane plus equipment) under control baseline conditions.

Results

Mass and plastron length of Sternotherus odoratus

The mass of each turtle was recorded upon arrival in the laboratory, and again on the date of use for electrophysiological recording. As one metric of good animal husbandry, it was noted that a majority of animals grew both in plastron length and in mass over their time in captivity (data not shown; usually 1–2 months). A variety of turtles, including musk turtles, are well-known to be sexually dimorphic in size as traditionally indexed by the length of the plastron (Ernst et al., 1994). Over our 4-year collection, female musk turtles had longer plastrons than males, reaching statistical significance in years 2003 and 2004 [Fig. 1A, two-way ANOVA,

Student–Neuman–Keuls (SNK) pairwise multiple comparison between sex and year, $P \leq 0.05$]. Using adult mass as a measure of dimorphism is not as reliable due to the fluctuation in the mass of the female during egg production (Fig. 1B).

Chemically activated properties

247 vomeronasal sensory neurons (VSNs) isolated from a total of 45 animals (31 females and 14 males) were tested for their ability to generate a current in response to stimulation with up to five different natural chemosignals (see Materials and methods; male musk, female musk, male urine, female urine and catfish extract). Each chemosignal was presented in the absence of the others, and the order of presentation was varied. Current responses of both inward and outward polarity typically rose to a maximum over several hundred milliseconds and subsequently declined to rest over a period of 3–4 s (Fig. 2). For all odor-exposure trials, neurons were clamped at a holding potential (V_h) of −60 mV, at which there is no voltage-gated channel activity. Eighty-eight of the 247 VSNs (35%) responded to the chemosignals presented (Fig. 3A). Of the 88 responsive VSNs, 40 (45%) responded to only one of the five chemicals presented in the array. The remaining VSNs (48 neurons, 55%) responded to between two and four of the five presented chemicals. None of the 88 VSNs responded to all five of the presented chemicals. The majority (64%) of VSNs responding to the tested chemosignals were isolated from female musk turtles due to animal collection bias, but females overall had a slightly lower response rate (defined by a response to at least one of the five chemicals presented; 34%) than did males (38%).

The recorded mean input resistance (R_N) of 2.9±0.3 GΩ (N=11) of VSNs at rest was similar to that previously recorded (Fadool et al., 2001) and also underscores the importance of small amplitude chemosignal-activated currents in these specialized sensory neurons. We have previously characterized the peak current response amplitudes for natural chemicals using an entropy (H metric) index from information theory that quantified the breadth of tuning for these neurons (Fadool et al., 2001). This study now furthers our initial characterization by exploring frequencies of response sorted to both sex and polarity. Here we report that chemosignal-activated currents can be of either polarity, depending on the cell and the chemosignal tested. Of the collective 165 responses generated by the 88 VSNs responding to chemosignals, outward currents were generated roughly twice as frequently as inward currents (107=outward responses; 58=inward responses; Fig. 3). The majority of chemosignals tested could evoke both inward and outward current dependent upon the individual VSN, but within a single VSN, a single chemosignal never elicited dual polarity, recording at a fixed command potential (V_c)=−60 mV. Most notably, a similar number of VSNs from females (17 cells, 30%) and males (6 cells, 20%) exhibited responses of both polarities when responsive to more than one chemosignal (data not shown). χ^2 analysis of the frequency pattern of outward and inward chemosignal-evoked current responses between male and female neurons indicated that the response pattern to male musk, male urine and catfish extract is statistically different across sex (Fig. 3B,D,F). More female neurons responded to male musk than did male neurons, but the response to female musk was not significantly different across sex (Fig. 3B,C; χ^2 analysis). Male urine evoked only outward currents in male VSNs (significantly different χ^2 analysis; Fig. 3D) but the response to female urine was not significantly different across sex (Fig. 3E). The stimulus most frequently eliciting a current response in both male and female VSNs was catfish extract (males, 47%; females, 50%) and female urine (males, 47%; females 40%) (Fig. 3E,F).

Chemosignal responses were examined in the absence of pharmacological agents for possible attenuation with repeated stimulation over time. In Fig. 4A (top trace), an isolated VSN was patch-clamped in the whole-cell configuration at a V_h of −60 mV. The VSN was then exposed to a 700 ms puff of chemosignal, denoted by the black bar above the recording. The cell was

then stimulated again at varying time intervals. The same chemosignal response 6 min after initial chemosignal exposure is shown in the bottom trace in Fig. 4A. As is shown in Fig. 4B, the normal chemosignal response was not altered over time (one-way repeated measures ANOVA, $P \leq 0.05$).

Ruthenium Red fails to alter chemosignal-activated currents, but a phospholipase C inhibitor reduces the chemosignal-activated current

Although IP_3R3 is expressed in the VNO of *Sternotherus odoratus* (J. H. Brann, unpublished data), it is not clear if it is found at the plasma membrane, as in olfactory cilia, or if it is restricted to the endoplasmic reticulum (ER). If a plasma membrane IP_3R has a direct role in the generation of a chemosignal-activated current, we reasoned that exposure to Ruthenium Red (RR), an IP_3R blocker, should reduce or alter that current. RR has been used to block IP_3-evoked currents in both the vomeronasal system and in the main olfactory system (Fadool and Ache, 1992; Miyamoto et al., 1992; Taniguchi et al., 1995; Kashiwayanagi et al., 2000). In this set of experiments, a baseline response to a given chemosignal was first obtained (defined as time 0, t_0), and 1 mmol l^{-1} RR was added to the bath surrounding the VSN. The chemosignal response was then recorded over the following 10 min (t_{10}) (Fig. 4C). Addition of RR to the bath did not alter the chemosignal response by 10 min (Fig. 4D; not significantly different, two-way repeated measures ANOVA, $P \leq 0.05$).

These experiments suggested that a plasma membrane IP_3R did not serve as the main carrier of the chemosignal-activated current in musk turtle VSNs, but two questions remained. First, it is not known whether the phospholipase C (PLC) system is required for the generation of chemosignal-activated currents in the musk turtle. Second, it is not clear what role, if any, the IP_3R may have in modulating the ion channel that is the primary carrier of the chemosignal-activated current. Therefore, a second set of VSNs were examined to investigate whether the chemosignal-activated current could be altered with the addition of a membrane-permeant phospholipase C inhibitor, U73122. Again, a baseline chemosignal response was obtained, 50 μmol l^{-1} U73122 was added to the bath, and chemosignal-activated current was monitored for the following 10 min (Fig. 4E). In this case, drug treatment with U73122 did rapidly (within 2 min) and significantly reduce the chemosignal-activated current, with the effect lasting for the duration of the test (Fig. 4F, significantly different, two-way repeated measures ANOVA, followed by SNK-pairwise multiple comparison between treatment and time, $P \leq 0.05$). The bath was not continually perfused, hence VSNs were not examined for washout recovery of the chemosignal-activated current. Neither the lack of response to RR (Fig. 4C,D) nor the reduction in current induced by U73122 (Fig. 4E,F) was dependent on current polarity, thus data were pooled for inward and outward current responses, and an example of each is demonstrated in the composition of this figure.

Second messenger analogues do not activate currents of either inward or outward polarity

Since the chemosignal-activated current was blocked by inhibiting phospholipase C, which would interfere with the generation of the two second messengers inositol 1,4,5-trisphosphate (IP_3) and diacylglycerol (DAG), we attempted to elicit currents that mimicked the chemosignal-activated current by including various second messenger analogues in the recording pipette while in the whole-cell configuration (Fig. 5). Fig. 5A is representative of recordings made at a V_h of −60 mV (below the threshold for voltage-activation). When 0.5 or 1 μmol l^{-1} cAMP, 240 μmol l^{-1} IP_3 or 125 μmol l^{-1} 1-oleoyl-2-acetyl-*sn*-glycerol (OAG; an analogue of DAG) were included in the patch pipette, no deflections were seen (Fig. 5B–D). A polyunsaturated fatty acid (PUFA) derivative of DAG, arachidonic acid (AA), was also included in the recording pipette, but failed to induce current fluctuations other than rare rapid transients (Fig. 5E). An additional, naturally occurring DAG analogue, SAG, was also tested (Fig. 5F). SAG did not elicit a chemosignal-like response, but did appear to make the membrane

unstable, probably due to its incorporation into the membrane. SAG was tested not only in the whole-cell configuration, but also on inside-out patches (N=4; data not shown), and in combination with IP_3 (N=5; data not shown), all of which failed to elicit chemosignal-like currents.

Reversal potential analysis supports a hypothesis of two chemosignal-activated conductances in the vomeronasal organ of S. odoratus

Since analogues failed to elicit chemosignal-like current, we tried to examine the ionic basis of the receptor potential as a means to gather evidence for a particular channel type in the formation of the chemosignal response in VSNs. We therefore characterized chemosignal-activated currents by means of reversal potential analysis. Representative examples of the reversal of an outward current (as defined by the polarity of the response at −60 mV) and an inward current are shown in Fig. 6A,B. The outward current depicted reversed at −20.8 mV, based upon a linear regression to the peak amplitude of the chemosignal-activated current at varying potentials (Fig. 6A,C). The inward current reversed at a similar potential, −27.9 mV (Fig. 6B,D). The average outward current reversed at −28.2±2.37 mV (means ± s.e.m.; N=30) and the inward current at −5.7±7.79 mV (N=10). The range of current reversals sorted per chemosignal are plotted in Fig. 6E,F for outward and inward polarity, respectively.

In addition to probing the reversal potential for the chemosignal response, we were interested in whether chemosignal application was accompanied by conductance changes in the VSN. If the chemosignal caused an ion channel to open, membrane resistance would decrease and conductance would increase, according to Ohm's Law and the calculated time constant. However, if an odorant caused an ion channel to close, exactly the opposite would occur, and conductance would decrease. Conductance changes were measured by injecting a series of five hyperpolarizing pulses from V_h=−60 mV to −90 mV (V_c) before, during and after chemosignal stimulation eliciting outward currents (Fig. 7). Chemosignal-evoked inward currents were not tested. At rest, VSNs had a mean input resistance (R_N) of 2.9±0.3 GΩ and a membrane time constant (τ) of 17.7±3.2 ms (N=11). Analysis of the current at the peak of the chemosignal response, when compared to the same hyperpolarizing step before and after chemosignal exposure, revealed a significant reduction in current (from 10.9±0.8 to 6.6±0.9 pA) and conductance (from 6.3±1.3 to 1.0±0.3 pS). In addition, a concomitant significant increase in R_N (5.7±0.9 GΩ) was seen as well as a significant decrease in τ to 4.3±1.2 ms (paired t-test, $P \leq 0.05$; Fig. 7).

A peptide directed against the TRPC2-IP_3R3 interaction domain blocks the chemosignal-activated current

We previously demonstrated that the ion channels TRPC2 and IP_3R3 participate in a protein–protein interaction in the VNO of the rat (Brann et al., 2002). The following experiments were designed to probe the question of a functional role of this protein–protein interaction, as well as to find possible common signal transduction mechanisms between the rat and the turtle. First, we sought to determine the functional role of the physical interaction between TRPC2 and IP_3R3. A recent publication using GST-fusion proteins of portions of these two channels demonstrated that calmodulin (CaM) and IP_3Rs share a common binding site on the carboxyl terminal of all TRPC channels (Tang et al., 2001). TRPC2 contains two such binding domains for CaM and all isoforms of the IP_3R, the first being amino acids 901–936, and the second being amino acids 942–1072. IP_3R3 also has a TRPC2 binding domain (amino acids 669–698) (Tang et al., 2001). We generated a peptide mimicking the first binding domain in the C terminus of TRPC2 (Fig. 8A), and included it in the patch pipette while recording from isolated VSNs in the whole-cell configuration and stimulating the VSN with a battery of different chemosignals (see Materials and methods). In all experiments, the designation 0 min is defined as the time at which the VSN was first exposed to a given chemosignal, or typically less than

30 s after breakthrough to the whole-cell configuration. A typical response from a VSN at 0 min is shown in the top trace of Fig. 8C. Inclusion of the peptide attenuated the chemosignal response within 5 min, with the effect lasting until 10 min (times later than 10 min were not tested) (Fig. 8B,C). Inclusion of boiled peptide in the recording pipette as a control did not alter the chemosignal response over 10 min (data not shown). Boiling results in denaturation of the peptide, and the peptide would presumably fail to bind the IP_3R, as has been demonstrated previously using similar peptide blocking approaches (Fadool and Ache, 1992; Holmes et al., 1996).

Discussion

Previously we had demonstrated sexual dimorphism in voltage-activated currents and somata size of VSNs isolated from the musk turtle, *S. odoratus*. In accordance with published data on the life history of this turtle species (Ernst et al., 1994), the female turtles in our trapped sample had longer plastrons than males. Because the VNO size can vary with age, reproductive cycle, season or mating strategy (Wilson and Raisman, 1980; Dawley and Crowder, 1995), it would be of interest to look at this variable in future studies where the organ was not harvested for electrophysiological analysis. In this study at the cellular level, we now demonstrate that chemosignal-activated currents show a degree of sexual dimorphism. In particular, we found that male VSNs responded more readily to female musk, while female VSNs responded more readily to male musk; both chemosignals could elicit either an inward or outward current, but not in the same VSN. While female urine and catfish extract elicited responses of both polarities equally well from both male and female VSNs, male VSNs responded to male urine with only an outward current. Current-clamp studies are needed to discern whether these chemosignals are altering action potential firing frequency (Moss et al., 1997; Inamura and Kashiwayanagi, 2000) and if there is evoked patterned activity that is sex specific.

Through our single cell-electrophysiology analysis, we found that several VSNs were found to respond to more than one chemosignal with opposite polarities of response. This may provide evidence for at least two signaling cascades in a single VSN. This assertion is supported by evidence that more than one G-protein-coupled receptor may be expressed in a single VSN (Martini et al., 2001; Spehr and Leinder-Zufall, 2005). Additionally, attempts to elicit chemosignal-activated currents outside the mating season (April–September) failed (J.H.B., unpublished). One might conjecture that not only size but also components of the cellular function of the VNO (or central projections) may be seasonally regulated.

The fact that Ruthenium Red (RR) did not significantly alter chemosignal-activated currents may suggest that IP_3R3 is not localized to the plasma membrane as has been demonstrated in cilia of olfactory sensory neurons (Fadool and Ache, 1992; Restrepo et al., 1992; Cunningham et al., 1993; Honda et al., 1995; Cadiou et al., 2000). These data, however, fail to reveal whether IP_3R3 is an important member of the signal transduction scaffold. RR is classically used as a blocker of the mitochondrial Ca^{2+} uniporter or of the ryanodine receptor (RyR) located on the ER. It has also been found, when applied extracellularly, to block the IP_3R localized to the dendrite or microvillus of an olfactory or vomeronasal sensory neuron, respectively (Fadool and Ache, 1992; Miyamoto et al., 1992; Taniguchi et al., 1995; Inamura et al., 1997; Taniguchi et al., 2000; Kashiwayanagi et al., 2000). An alternative possibility that must be considered is that the TRPC2/IP_3R3 complex may present a configuration that is inaccessible for pharmacological interception with RR.

This study provides the first evidence that dissociated VSNs from the semi-aquatic turtle, *S. odoratus*, utilize the phospholipase C (PLC) system in the detection of socially relevant stimuli. A membrane-permeable inhibitor of PLC, U73122, significantly reduced the chemosignal-activated current. These data support the hypothesis that the phosphatidylinositol system

underlies the chemosignal response in VSNs. However, it is not clear whether the derivatives of PIP_2, DAG or IP_3, have a direct role in gating the ion channels involved. In guinea pig ileal smooth muscle cells, the activation of the muscarinic receptor-operated cationic current (likely *via* a TRP channel), is dependent upon PLC, but is not dependent on either IP_3 or DAG (Zholos et al., 2004). PIP_2 may directly modulate the TRP channel in question, as is seen with TRPM5, TRPM7, TRPM7 and TRPV1 (Hilgemann et al., 2001; Liu and Qin, 2005; Chuang et al., 2001; Liu and Liman, 2003; Prescott and Julius, 2003). In these cases, PIP_2 sometimes acts to suppress channel activity. Interestingly, when mutations are made within the PIP_2 binding domain on TRPV1, the channel becomes more sensitive to chemical or thermal stimuli (Prescott and Julius, 2003). In the case of TRPM5 and TRPM8, PIP_2 activates the channel. PIP_2 can reverse the desensitization of TRPM5 (Liu and Liman, 2003). Blocking PIP_2 synthesis inhibits TRPM8 activity (Liu and Qin, 2005). Therefore, PIP_2 has the potential to differentially and directly regulate several members of the TRP ion channel superfamily, and may be directly modulating TRPC2 current in the VNO, either directly affecting the primary receptor potential, or perhaps the formation of a signal complex with IP_3R3.

Using our experimental design, dialysis with the second messengers cAMP, IP_3 or DAG failed to elicit a response in isolated VSNs. Although cAMP did not have an effect, other cyclic nucleotides could be important in a transduction pathway in the musk turtle VNO (Taniguchi et al., 1996). The lack of response with dialyzed messengers could be explained in several ways. First, the whole-cell patch seal was formed on the soma, not on the thin dendritic extension or microvilli. Thus it is possible that the messengers may not have reached a critical concentration near the transduction apparatus in the microvilli (Berghard and Buck, 1996; Ryba and Tirindelli, 1997; Liman et al., 1999; Menco et al., 2001). Contrary to this explanation is that soma dialysis of second messengers by one of the authors has been shown to evoke quite large currents in olfactory sensory neurons of lobster with outer dendrites (primary site of transduction) greater than 1000 μm from the cell body (Fadool and Ache, 1992). This space problem was apparently alleviated in frog VSNs by using flash photolysis of caged IP_3, and selective release of IP_3 only near the microvillus resulted in a series of transient inward currents when the membrane was held at −70 mV (Gjerstad et al., 2003). Second, the VSNs studied here were enzymatically isolated, and may have altered the ability of the VSN to respond to dialyzed second messenger; however, this is less likely because VSNs isolated in the same manner were shown to be responsive to chemosignals, and cells lacking microvilli were not included in the current study. Third, PIP_2 could interact directly with TRPC2 in the musk turtle, bypassing the need for either IP_3 or DAG, as discussed above. Another possibility is that DAG and IP_3 must be presented in tandem for effects to be detected; such synergism in the generation of a non-selective cationic current has been demonstrated in rabbit portal vein myocytes (Albert and Large, 2003). This hypothesis was informally tested here yet the combined presentation of IP_3 and the DAG analogue, SAG, did not elicit currents of either inward or outward polarity. Finally, arachidonic acid, a polyunsaturated acid (PUFA) derived from DAG previously reported to generate chemosignal-like currents in the rat vomeronasal system (Spehr et al., 2002), did not elicit chemosignal-like currents in isolated *S. odoratus* VSNs but did appear to evoke rapid transients, the function of which is unclear.

Two separate reversal potentials for inward and outward currents were revealed. The majority of chemosignals, with the exception of male urine, were capable of eliciting both polarities of response; hence, most chemosignals did not appear to be stereotypically connected to a particular signal transduction cascade. Male urine, however, may be operating exclusively as a territorial cue, and the receptive pathway for such information may be stereotyped. The outward current, reversing at approximately −30 mV, may be due to the closure of an ion channel of unknown identity. Although a novel transduction mechanism in the musk turtle VNO, such a channel operates in several sensory organs, including the visual system and the mouse VNO (Matesic and Liebman, 1987; Moss et al., 1997). The inward current reversed

close to 0 mV, indicating that this current is due to a nonselective cation channel, such as TRPC2. A good future directive would be to explore whether the musk turtle VNO may express a Ca^{2+}-activated non-selective (CaNS) cation channel like that found in the hamster (Liman, 2003), or a Ca^{2+}-activated chloride channel, similar to that seen in olfactory sensory neurons that would contribute a late-phase amplification of the initial Ca^{2+} current (Kleene, 1993; Lowe and Gold, 1993; Paysan and Breer, 2001).

The interaction between TRPC channels and the IP_3R has been well established (Tang et al., 2001; Yuan et al., 2003; Brann et al., 2002). Here, we sought to demonstrate a role for this interaction in the VNO of the musk turtle. Recent GST-fusion work has shown (Tang et al., 2001) that IP_3R3 and calmodulin bind to a conserved amino acid sequence found on most TRPC channels, including mTRPC2 (mouse TRPC2; amino acids 901–936). mTRPC2 appears to be somewhat unique within the canonical TRP superfamily in that it possesses an additional binding site (amino acids 944–1072) (Tang et al., 2001). We designed a peptide (see Materials and methods) against this sequence to interrupt the binding of IP_3R3 to TRPC2 and analyzed its effect on the chemosignal response over time in musk turtle VSNs, and found that 10 μmol l^{-1} peptide nearly abolished the chemosignal-activated current by 10 min. The use of a peptide to disrupt the interaction between the IP_3R and a TRPC channel has been shown previously; in *Xenopus* oocytes, suppression of the mTRPC5 current was seen with preinjection of a peptide mimicking the IP_3 binding domain of the IP_3R (Kanki et al., 2001). These results indicate that there is a functional role for the IP_3R in the VNO of the musk turtle. Since dialysis of IP_3 did not elicit a current alone, it is possible that the IP_3R is serving to amplify the initial receptor potential generated by TRPC2, to achieve sensitivity to repeated stimulation with chemosignal, or to modulate seasonality in this species. It is also possible that when IP3R/TRPC2 are in a complex, the IP3 ligand could have less affinity or lack access to the receptor. This later possibility would be consistent with our data that demonstrate a lack of current after IP3 dialysis and failure of an IP3R antagonist (RR) to significantly block chemosignal-activated current.

The experiments presented here demonstrate that the PLC system is required in VSNs from *S. odoratus* to detect a variety of natural chemical cues, including urine and a reproductive musk known to mediate mating behaviors/courtship (Eisner et al., 1977). This finding is consistent with studies in the rodent (Spehr et al., 2002; Lucas et al., 2003). In addition, it is likely that the TRPC2-IP_3R3 protein–protein interaction previously demonstrated in rodent (Brann et al., 2002) does have a functional role in the chemosignal response of VSNs, as interrupting the interaction resulted in loss of the chemosignal response. These data imply that the connection between the internal Ca^{2+} stores is important to the maintenance of the response in the VNO, and may have a role in the ability of the VNO to respond to chemosignals repetitively without a decrease in action potential firing frequency, a property that is not found in the main olfactory system (Liman and Corey, 1996). Although second messenger dialysis failed to elicit a chemosignal-like current, reversal potential analysis supports the existence of a conductance consistent with a nonspecific cation channel such as TRPC2, the expression of which was found in *S. odoratus* previously (Murphy et al., 2001). One very interesting result of these studies was that outward currents (as defined at −60 mV) may be due to the closure of an inwardly conducting ion channel. This is not the first report of such a channel in the VNO (Moss et al., 1997; Moss et al., 1998), although it is the first report in the turtle.

List of abbreviations

AA, arachidonic acid
AOS, accessory olfactory system
ANOVA, analysis of variance
CaM, calmodulin
cAMP, cyclic adenosine monophosphate

CaNS, Ca^{2+}-activated non-selective
DAG, diacylglycerol
ER, endoplasmic reticulum
GPCR, G-protein-coupled receptor
IP_3, inositol 1,4,5-trisphosphate
IP_3R, IP_3 receptor
IP_3R3, type 3 IP_3 receptor
MOE, main olfactory epithelium
MOS, main olfactory system
OAG, 1-oleoyl-2-acetyl-*sn*-glycerol
PBS, phosphate buffered saline
PIP_2, phosphatidyl-inositol bis-phosphate
PLC, phospholipase C
PUFA, polyunsaturated fatty acid
R_N, input resistance
RR, Ruthenium Red
RT, room temperature
RyR, ryanodine receptor
SAG, 1-stearoyl-2-arachidonoyl-*sn*-glycerol
SNK, Student–Newman–Keuls
t_0, first exposure to chemosignal
t_n, exposure to chemosignal at time n
t_p, time point
TRPC2, canonical transient receptor potential 2
V_c, command potential
V_h, holding potential
VNO, vomeronasal organ
VSN, vomeronasal sensory neuron
U73122, PLC inhibitor
τ, time constant

Acknowledgments

J.H.B. was supported by a NIH/NIDCD Ruth L. Kirschstein National Research Service Award (NRSA) F31-DC006153 and by a NIH/NIDCD Predoctoral Chemosensory Training Grant T32-DC00044 to the Florida State University. We would like to thank Drs Francis Rose, Mary Mendonca and Craig Guyer for the donation and collection of animals. We would also like to thank Mr Roger Thompson, Mr Chad Thorson, and Ms Randa Perkins for invaluable field assistance.

References

Albert AP, Large WA. Synergism between inositol phosphates and diacylglycerol on native TRPC6-like channels in rabbit portal vein myocytes. J. Physiol 2003;522:789–795. [PubMed: 12972630]

Baxi KN, Dorries KM, Eisthen HL. Is the vomeronasal system really specialized for detecting pheromones? Trends Neurosci 2006;29:1–7. [PubMed: 16271402]

Berghard A, Buck LB. Sensory transduction in vomeronasal neurons: evidence for G alpha o, G alpha i2, and adenylyl cyclase II as major components of a pheromone signaling cascade. J. Neurosci 1996;16:909–918. [PubMed: 8558259]

Berridge MJ, Irvine RF. Inositol trisphosphate, a novel second messenger in cellular signal transduction. Nature 1984;312:315–321. [PubMed: 6095092]

Brann JH, Dennis JC, Morrison EE, Fadool DA. Type specific inositol 1,4,5-trisphosphate receptor localization in the vomeronasal organ and its interaction with a transient receptor potential channel, TRPC2. J. Neurochem 2002;83:1452–1460. [PubMed: 12472899]

Cadiou H, Sienaert I, Vanlingen S, Parys JB, Molle G, Duclohier H. Basic properities of an inositol 1,4,5-trisphosphategated channel in carp olfactory cilia. Eur. J. Neurosci 2000;12:2805–2811. [PubMed: 10971622]

Clapham DE, Runnels LW, Strubing C. The TRP ion channel family. Nat. Rev. Neurosci 2001;80:387–396. [PubMed: 11389472]

Chyb S, Raghu P, Hardie RC. Polyunsaturated fatty acids activate the Drosophila light-sensitive channels TRP and TRPL. Nature 1999;397:255–259. [PubMed: 9930700]

Chuang HH, Prescott ED, Kong H, Shields S, Jordt SE, Basbaum AI, Chao MV, Julius D. Bradykinin and nerve growth factor release the capsaicin receptor from PtdIns(4,5)P2-mediated inhibition. Nature 2001;411:957–962. [PubMed: 11418861]

Cunningham AM, Ryugo DK, Sharp AH, Reed RR, Snyder SH, Ronnett GV. Neuronal inositol 1,4,5-trisphosphate receptor localized to the plasma membrane of olfactory cilia. Neuroscience 1993;57:339–352. [PubMed: 8115043]

Dawley EM. Species, sex, and seasonal differences in VNO size. Microsc. Res. Tech 1998;41:506–518. [PubMed: 9712198]

Dawley EM, Crowder J. Sexual and seasonal differences in the vomeronasal epithelium of the red-backed salamander (*Plethdon cinereus*). J. Comp. Neurol 1995;359:382–390. [PubMed: 7499536]

Dulac C, Axel R. A novel family of genes encoding putative pheromone receptors in mammals. Cell 1995;83:195–206. [PubMed: 7585937]

Eisner T, Conner WE, Hicks K, Dodge KR, Rosenberg HI, Jones TH, Cohen M, Meinwald J. Stink of stinkpot turtles identified: O-phenylalkanoic acids. Science 1977;196:1347–1349. [PubMed: 17831752]

Ernst, CH.; Lovich, JE.; Barbour, RW. Turtles of the United States and Canada. Washington: Smithsonian Institute Press; 1994.

Fadool DA, Ache BW. Plasma membrane inositol 1,4,5-trisphosphate-activated channels mediate signal transduction in lobster olfactory receptor neurons. Neuron 1992;9:907–918. [PubMed: 1384577]

Fadool DA, Wachowiak M, Brann JH. Patch-clamp analysis of voltage-activated and chemically activated currents in the vomeronasal organ of *Sternotherus odoratus* (stinkpot/musk turtle). J. Exp. Biol 2001;204:4199–4212. [PubMed: 11815645]

Firestein S, Werblin F. Odor-induced membrane currents in vertebrate-olfactory receptor neurons. Science 1989;244:79–82. [PubMed: 2704991]

Gjerstad J, Valen EC, Trotier D, Døving K. Photolysis of caged inositol 1,4,5-trisphosphate induces action potentials in frog vomeronasal microvillar receptor neurons. Neuroscience 2003;119:193–200. [PubMed: 12763080]

Halpern M, Martínez-Marcos A. Structure and function of the vomeronasal system: an update. Prog. Neurobiol 2003;70:245–318. [PubMed: 12951145]

Hamill OP, Marty A, Neher E, Sakmann B, Sigworth FJ. Improved patchclamp techniques for high-resolution current recording from cells and cell-free membrane patches. Pflügers Arch 1981;391:85–100.

Herrada G, Dulac C. A novel family of putative pheromone receptors in mammals with a topographically organized and sexually dimorphic distribution. Cell 1997;90:763–773. [PubMed: 9288755]

Hilgemann DW, Feng S, Nasuhoglu C. The complex and intriguing lives of PIP2 with ion channels and transporters. Sci. STKE 2001;2001:RE19. [PubMed: 11734659]

Hirokawa T, Boon-Chieng S, Mitaku S. SOSUI: classification and secondary structure prediction system of membrane proteins. Bioinformatics 1998;14:378–379. [PubMed: 9632836]

Hoffman K, Stoffel W. TMbase - a database of membrane spanning protein segments. Biol. Chem 1993;374:166.

Hofmann T, Obukhov AG, Schaefer M, Harteneck C, Gudermann T, Schultz G. Direct activation of human TRPC6 and TRPC3 channels by diacylglycerol. Nature 1999;397:259–263. [PubMed: 9930701]

Holmes TC, Fadool DA, Ren R, Levitan IB. Association of Src tyrosine kinase with a human potasssium channel medicate by SH3 domain. Science 1996;274:2089–2091. [PubMed: 8953041]

Honda E, Teeter JH, Restrepo D. InsP3-gated ion channels in rat olfactory cilia membrane. Brain Res 1995;703:79–85. [PubMed: 8719618]

Inamura K, Kashiwayanagi M. Inward current responses to urinary substances in rat vomeronasal sensory neurons. Eur. J. Neurosci 2000;12:3529–3536. [PubMed: 11029622]

Inamura K, Kashiwayanagi M, Kurihara K. Blockage of urinary responses by inhibitors for IP_3-mediated pathway in rat vomeronasal sensory neurons. Neurosci. Lett 1997;233:129–132. [PubMed: 9350849]

Kanki H, Kinoshita M, Akaike A, Satoh M, Mori Y, Kaneko S. Activation of inositol 1,4,5-trisphosphate receptor is essential for the opening of mouse TRP5 channels. Mol. Pharmacol 2001;60:989–998. [PubMed: 11641427]

Karlson P, Lüscher M. 'Pheromones': a new term for a class of biologically active substances. Nature 1959;183:55–56. [PubMed: 13622694]

Kashiwayanagi M, Tatani K, Shuto S, Matsuda A. Inositol 1,4,5-trisphosphate and adenophostin analogues induce responses in turtle olfactory sensory neurons. Eur. J. Neurosci 2000;12:606–612. [PubMed: 10712640]

Kleene SJ. Origin of the chloride current in olfactory transduction. Neuron 1993;11:123–132. [PubMed: 8393322]

Labra A, Brann JH, Fadool D. Heterogeneity of voltage-and chemosignal-activated response profiles in vomeronasal sensory neurons. J. Neurophysiol 2005;94:2535–2548. [PubMed: 15972830]

Leinders-Zufall T, Rand MN, Shepherd GM, Greer CA, Zufall F. Calcium entry through cyclic nucleotide-gated channels in individual cilia of olfactory receptor cells: spatiotemporal dynamics. J. Neurosci 1997;17:4136–4148. [PubMed: 9151731]

Leinders-Zufall T, Brennan P, Widmayer P, Chandramani PS, Maul-Pavicic A, Jäger M, Li X-H, Breer H, Zufall F, Boehm T. MHC class I peptides as chemosensory signals in the vomeronasal organ. Science 2004;306:1033–1036. [PubMed: 15528444]

Leypold BG, Yu CR, Leinders-Zufall T, Kim MM, Zufall F, Axel R. Altered sexual and social behaviors in trp2 mutant mice. Proc. Natl. Acad. Sci. USA 2002;99:6376–6381. [PubMed: 11972034]

Liman ER. Regulation by voltage and adenine nucleotides of a Ca^{2+}-activated cation channel from hamster vomeronasal sensory neurons. J Physiol 2003;14:777–787. [PubMed: 12640014]

Liman ER, Corey DP. Electrophysiological characterization of chemosensory neurons from the mouse vomeronasal organ. J. Neurosci 1996;16:4625–4637. [PubMed: 8764651]

Liman ER, Corey DP, Dulac C. TRPC2: a candidate transduction channel for mammalian pheromone sensory signaling. Proc. Natl. Acad. Sci. USA 1999;96:5791–5796. [PubMed: 10318963]

Liu B, Qin F. Functional control of cold- and menthol-sensitive TRPM8 ion channels by phosphatidylinositol 4,5-bisphosphate. J. Neurosci 2005;25:1674–1681. [PubMed: 15716403]

Liu D, Liman ER. Intracellular Ca^{2+} and the phospholipid PIP_2 regulate the taste transduction ion channel TRPM5. Proc. Natl. Acad. Sci. USA 2003;100:15160–15165. [PubMed: 14657398]

Lowe G, Gold GH. Nonlinear amplification by calcium-dependent chloride channels in olfactory receptor cells. Nature 1993;366:283–286. [PubMed: 8232590]

Lucas P, Uhkanov K, Leinders-Zufall T, Zufall Z. A diacylglycerol-gated cation channel in vomeronasal neuron dendrites is impaired in *TRPC2* mutant mice. Neuron 2003;40:551–561. [PubMed: 14642279]

Martini S, Silvotti L, Shirazi A, Ryba NJ, Tirindelli R. Co-expression of putative pheromone receptors in the sensory neurons of the vomeronasal organ. J. Neurosci 2001;21:843–848. [PubMed: 11157070]

Matesic D, Liebman PA. cGMP-dependent cation channel of retinal rod outer segments. Nature 1987;326:600–603. [PubMed: 2436056]

Matsunami H, Buck LB. A multigene family encoding a diverse array of putative pheromone receptors in mammals. Cell 1997;90:775–784. [PubMed: 9288756]

Menco BP, Carr VM, Ezeh PI, Liman ER, Yankova MP. Ultrastructural localization of G-proteins and the channel protein TRPC2 to microvilli of rat vomeronasal receptor cells. J. Comp. Neurol 2001;438:468–489. [PubMed: 11559902]

Meredith M. Sensory processing in the main and accessory olfactory systems: comparisons and contrasts. J. Steroid Biochem. Mol. Biol 1991;39:601–614. [PubMed: 1892791]

Meredith M. Human vomeronasal organ function: a critical review of best and worst cases. Chem. Senses 2001;26:433–445. [PubMed: 11369678]

Minke B, Cook B. TRP channel proteins and signal transduction. Physiol. Rev 2002;82:429–472. [PubMed: 11917094]

Mittman SC, Flaming DG, Copenhagen DR, Belgum JH. Bubble pressure measurement of micropipet tip outer diameter. J. Neurosci. Methods 1987;22:161–166. [PubMed: 3437778]

Miyamoto T, Restrepo D, Cragoe EJ Jr, Teeter JH. IP3-and cAMP-induced responses in isolated olfactory receptor neurons from the channel catfish. J. Membr. Biol 1992;127:173–183. [PubMed: 1379643]

Moss RL, Flynn RE, Shen X-M, Dudley C, Shi J, Novotny M. Urine-derived compound evokes membrane responses in mouse vomeronasal receptor neurons. J. Neurophysiol 1997;77:2856–2862. [PubMed: 9163402]

Moss RL, Flynn RE, Shi J, Shen X-M, Dudley C, Zhou A, Novotny M. Electrophysiological and biochemical responses of mouse vomeronasal receptor cells to urine-derived compounds: possible mechanism of action. Chem. Senses 1998;23:483–489. [PubMed: 9759537]

Murphy FA, Tucker K, Fadool DA. Sexual dimorphism and developmental expression of signal transduction machinery in the vomeronasal organ. J. Comp. Neurol 2001;432:61–74. [PubMed: 11241377]

O'Connell RJ, Meredith M. Effects of volatile and nonvolatile chemical signals on male sex behaviors mediated by the main and accessory olfactory systems. Behav. Neurosci 1984;98:1083–1093. [PubMed: 6508913]

Pantages E, Dulac C. A novel multigene family of candidate pheromone receptors in mammals. Neuron 2000;28:835–845. [PubMed: 11163270]

Paysan J, Breer H. Molecular physiology of odor detection: current views. Pflugers Arch 2001;441:579–586. [PubMed: 11294238]

Pocock TM, Foster RR, Bates DO. Evidence of a role for TRPC channels in VEGF-mediated increased vascular permeability *in vivo*. Am. J. Physiol 2004;286:H1015–H1026.

Prescott ED, Julius D. A modular PIP2 binding site as a determinant of capsaicin receptor sensitivity. Science 2003;300:1284–1288. [PubMed: 12764195]

Restrepo D, Teeter JH, Honda E, Boyle AG, Marecek JF, Prestwich GD, Kalinoski DL. Evidence for an InsP3-gated channel protein in isolated rat olfactory cilia. Am. J. Physiol 1992;263:C667–C673. [PubMed: 1384346]

Restrepo D, Arellano J, Oliva AM, Schaefer ML, Lin W. Emerging views on the distinct but related roles of the main and accessory olfactory systems in responsiveness to chemosensory signals in mice. Horm. Behav 2004;46:247–256. [PubMed: 15325226]

Rodriguez I, Punta KD, Rothman A, Ishii T, Mombaerts P. Multiple new and isolated families within the mouse superfamily of V1r vomeronasal receptors. Nat. Neurosci 2002;5:134–140. [PubMed: 11802169]

Runnenburger K, Breer H, Boekhoff I. Selective G protein beta gamma-subunit compositions mediate phospholipase C activation in the vomeronasal organ. Eur. J. Cell Biol 2002;81:539–547. [PubMed: 12437188]

Ryba NJ, Tirindelli R. A new multigene family of putative pheromone receptors. Neuron 1997;19:371–379. [PubMed: 9292726]

Spehr M, Leinder-Zufall T. One neuron – multiple receptors: increased complexity in olfactory coding? Sci. STKE 2005;2005:pe25. [PubMed: 15914726]

Spehr M, Hatt H, Wetzel CH. Arachidonic acid plays a role in rat vomeronasal signal transduction. J. Neurosci 2002;22:8429–8437. [PubMed: 12351717]

Steel, RGD.; Torrie, JH. Principles and Procedures of Statistics: A Biometrical Approach. New York: McGraw Hill; 1980.

Stowers L, Holy TE, Meister M, Dulac C, Koentges G. Loss of sex determination and male-male aggression in mice deficient for TRP2. Science 2002;295:1493–1500. [PubMed: 11823606]

Tang J, Lin Y, Zhang Z, Tikunova S, Birnbaumer L, Zhu MX. Identification of common binding sites for calmodulin and IP3 receptors on the Carboxyl-termini of Trp channels. J. Biol. Chem 2001;276:21303–21310. [PubMed: 11290752]

Taniguchi M, Kashiwayanagi M, Kurihara K. Intracellular injection of inositol 1,4,5-trisphosphate increases a conductance in membranes of turtle vomeronasal receptor neurons in the slice preparation. Neurosci. Lett 1995;188:5–8. [PubMed: 7540275]

Taniguchi M, Kashiwayanagi M, Kurihara K. Intracellular dialysis of cyclic nucleotides induces inward currents in turtle vomeronasal receptor neurons. J. Neurosci 1996;16:1239–1246. [PubMed: 8558252]

Taniguchi M, Wang D, Halpern M. Chemosensitive conductance and inositol 1,4,5-trisphosphate-induced conductance in snake vomeronasal receptor neurons. Chem. Senses 2000;25:67–76. [PubMed: 10667996]

Trinh K, Storm DR. Vomeronasal organ detects odorants in absence of signaling through main olfactory epithelium. Nat. Neurosci 2003;6:519–525. [PubMed: 12665798]

Vannier B, Peyton M, Boulay G, Brown D, Qin N, Jiang M, Zhu X, Birnbaumer L. Mouse trp2, the homologue of the human trpc2 pseudogene, encodes mTrp2, a store depletion-activated capacitative Ca^{2+} entry channel. Proc. Natl. Acad. Sci. USA 1999;96:2060–2064. [PubMed: 10051594]

Venkatachalam K, Ma HT, Ford DL, Gill DL. Expression of functional receptor-coupled TRPC3 channels in DT40 triple receptor InsP3 knockout cells. J. Biol. Chem 2001;276:33980–33985. [PubMed: 11466302]

Venkatachalam K, Zheng F, Gill DL. Regulation of canonical transient receptor potential (TRPC) channel function by diacylglycerol and protein kinase C. J. Biol. Chem 2003;278:29031–29040. [PubMed: 12721302]

Vitt LJ, Pianka ER, Cooper WE Jr, Schwenk K. History and the global ecology of squamate reptiles. Am. Nat 2003;162:44–60. [PubMed: 12856236]

Vogt RG, Vieyra M, Anderson D. New discoveries in the olfactory capability of sea turtles. Pelagic Fish. Res. Prog 2002;7:6–9.

Wang D, Chen P, Liu W, Li CS, Halpern M. Chemosignal transduction in vomeronasal organ of garter snakes: Ca(2+)-dependent regulation of adenylate cyclase. Arch. Biochem. Biophys 1997;348:96–106. [PubMed: 9390179]

Wilson KC, Raisman G. Age-related changes in the neurosensory epithelium of the mouse vomeronasal organ: extended period of postnatal growth in size and evidence for rapid cell turnover in the adult. Brain Res 1980;185:103–113. [PubMed: 7353170]

Yuan JP, Kiselyov K, Shin DM, Chen J, Shcheynikov N, Kang SH, Dehoff MH, Schwarz MK, Seeburg PH, Muallem S, et al. Homer binds TRPC family channels and is required for gating of TRPC1 by IP3 receptors. Cell 2003;114:777–789. [PubMed: 14505576]

Zholos AV, Tsytsyura YD, Gordienko DV, Tsvilovskyy VV, Bolton TB. Phospholipase C, but not InsP3 or DAG, -dependent activation of the muscarinic receptor-operated cation current in guinea-pig ileal smooth muscle cells. Br. J. Pharmacol 2004;1:23–36. [PubMed: 14662735]

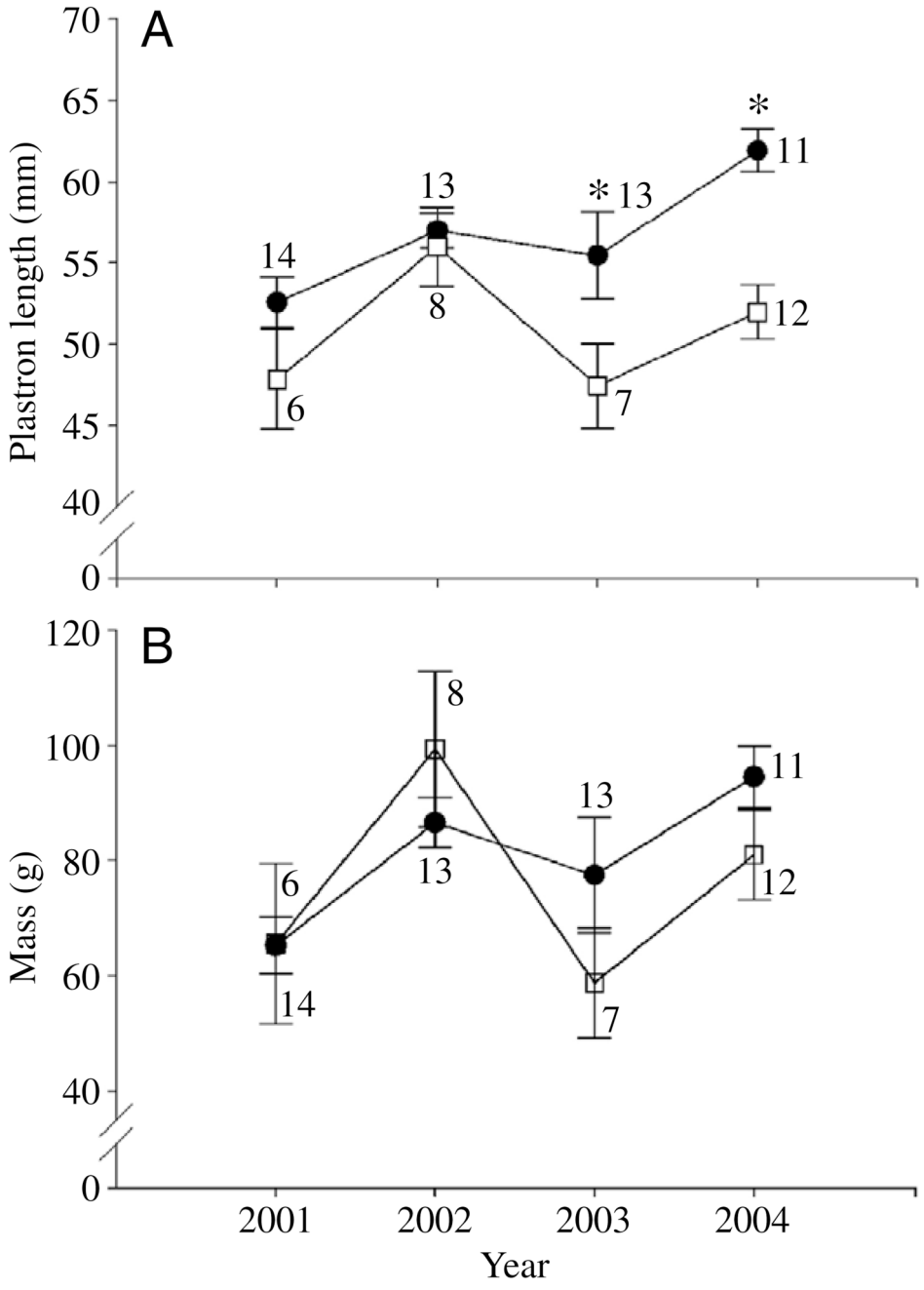

Fig. 1.

Plastron length and mass of *Sternotherus odoratus*, by year. (A) Adult female (filled circles) *versus* adult male (open squares) plastron length, *S. odoratus versus* collection year (asterisk denotes significantly different between sexes in years shown; mean ± s.e.m.; two-way ANOVA, SNK pairwise multiple comparison between sex and year, $P \leq 0.05$). (B) Mass of adult female (filled circles) and male (open squares) *Sternotherus odoratus versus* collection year (not significantly different; mean ± s.e.m.; two-way ANOVA, $P \leq 0.05$). *N* values are shown beside symbols.

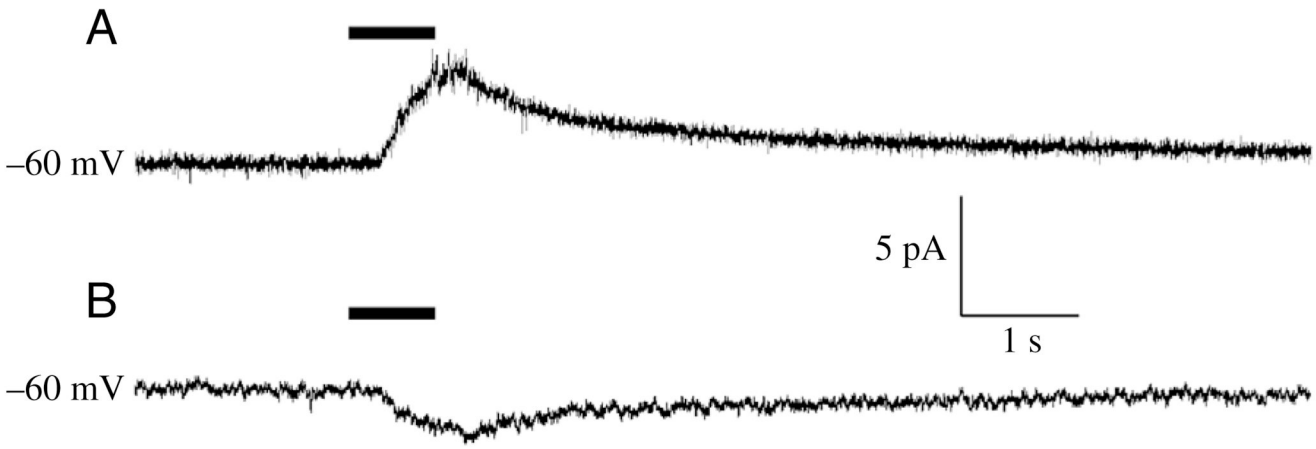

Fig. 2.

Representative examples of chemosignal-activated current obtained with chemical stimulation of vomeronasal sensory neurons (VSNs). (A) A male vomeronasal sensory neuron (VSN) when stimulated with catfish extract exhibited an outward current, as defined by the polarity of the response obtained at holding potential V_h=−60 mV. The black bar above the trace denotes the time (700 ms) that the VSN was presented with chemosignal delivered *via* a pressurized glass pipette approximately two cell-widths away from the VSN. (B) As in A but for a female VSN stimulated with female musk. Current record is representative of an inward current, as defined by the polarity of the response obtained at V_h=−60 mV.

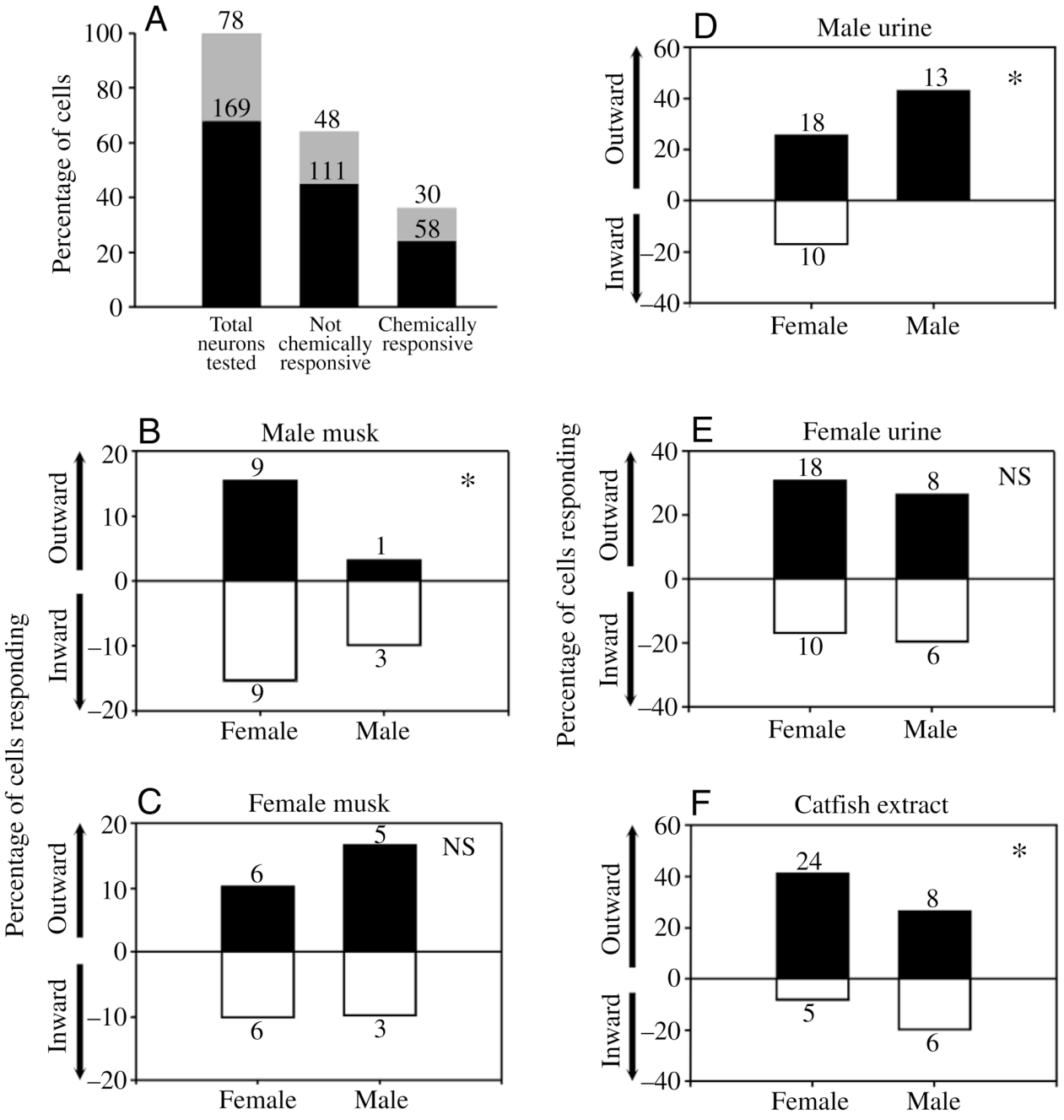

Fig. 3.

The percentage of cells responding with a given polarity to a particular chemosignal is different between male and female vomeronasal sensory neurons (VSNs). (A) Histogram plot of the three different response categories of VSNs, separated on the basis of sex; male, gray; female, black. (B–F) Histogram plots of the percentage of female and male VSNs responding with an outward (black bars) or inward (white bars) current to (B) male musk, (C) female musk, (D) male urine, (E) female urine, (F) catfish extract. *Significantly different response frequency of inward and outward current across sex by χ^2 analysis, $P \leq 0.05$; NS, not significantly different. *N* values are shown beside bars.

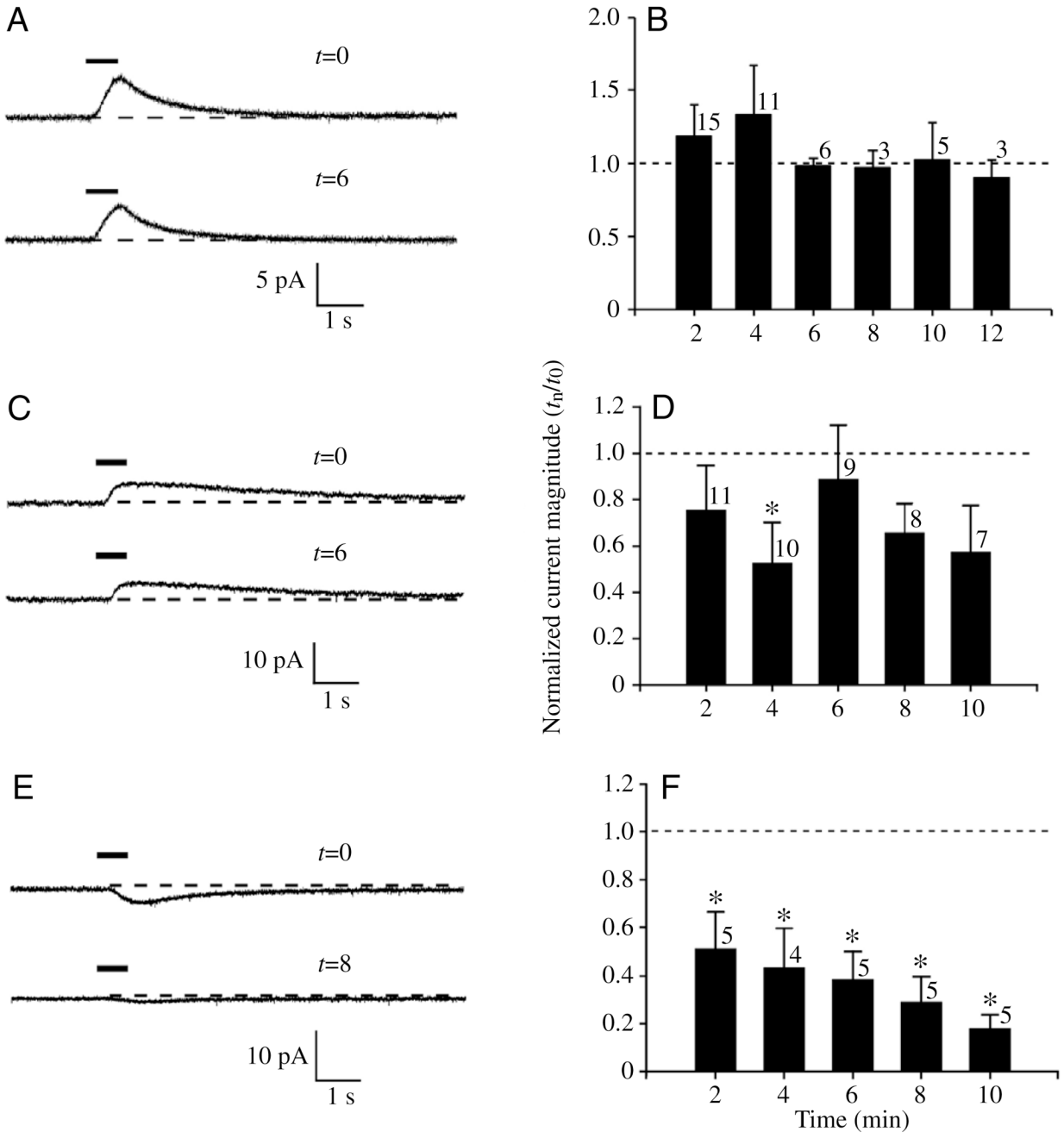

Fig. 4.

Ruthenium Red (RR), an antagonist of the IP_3R, fails to block chemosignal-activated currents in *S. odoratus* vomeronasal sensory neurons (VSNs) while an inhibitor of phospholipase C (U73122) does block chemosignal-activated currents. (A) A representative example of the response of a female VSN to catfish extract at 0 min (top trace) and 6 min later (bottom trace) without pharmacological perturbation. The chemosignal presentation is shown as black bar above the response. This particular cell was used primarily for reversal potential analysis, hence the VSN had been exposed to the chemical signal twelve times within the time span described. (B) Histogram plot of the normalized current magnitude (normalized to first exposure to chemosignal; t_0) over time. Cells were sampled at varying time points (t_n), such that not every

cell was sampled for each of the time points. The amplitude of the chemosignal-activated current was not altered over 12 min (one-way repeated measures ANOVA, $P \leq 0.05$). (C) A representative example of the response of a female VSN to male urine at 0 min (top trace) and 6 min (bottom trace) following bath application of 1 mmol 1^{-1} RR. (D) Histogram plot of the normalized current magnitude (normalized to t_0) over time. The chemosignal-activated current is not altered over 10 min (not significantly different by treatment or time, two-way repeated measures ANOVA, $P \leq 0.05$) in response to RR treatment. The normal chemosignal response over time is denoted by the broken line. (E) A representative example of the response of a female VSN to catfish extract at 0 min (top trace) and 8 min (bottom trace) following bath application of 50 μmol l^{-1} U73122. (F) As in D but for U73122 treatment. Asterisks denote significant difference between treatments, two-way repeated measures ANOVA, followed by SNK pairwise multiple comparison between treatment and time, $P \leq 0.05$). *N* values are shown beside bars. (A,C,E) Broken line denotes baseline current.

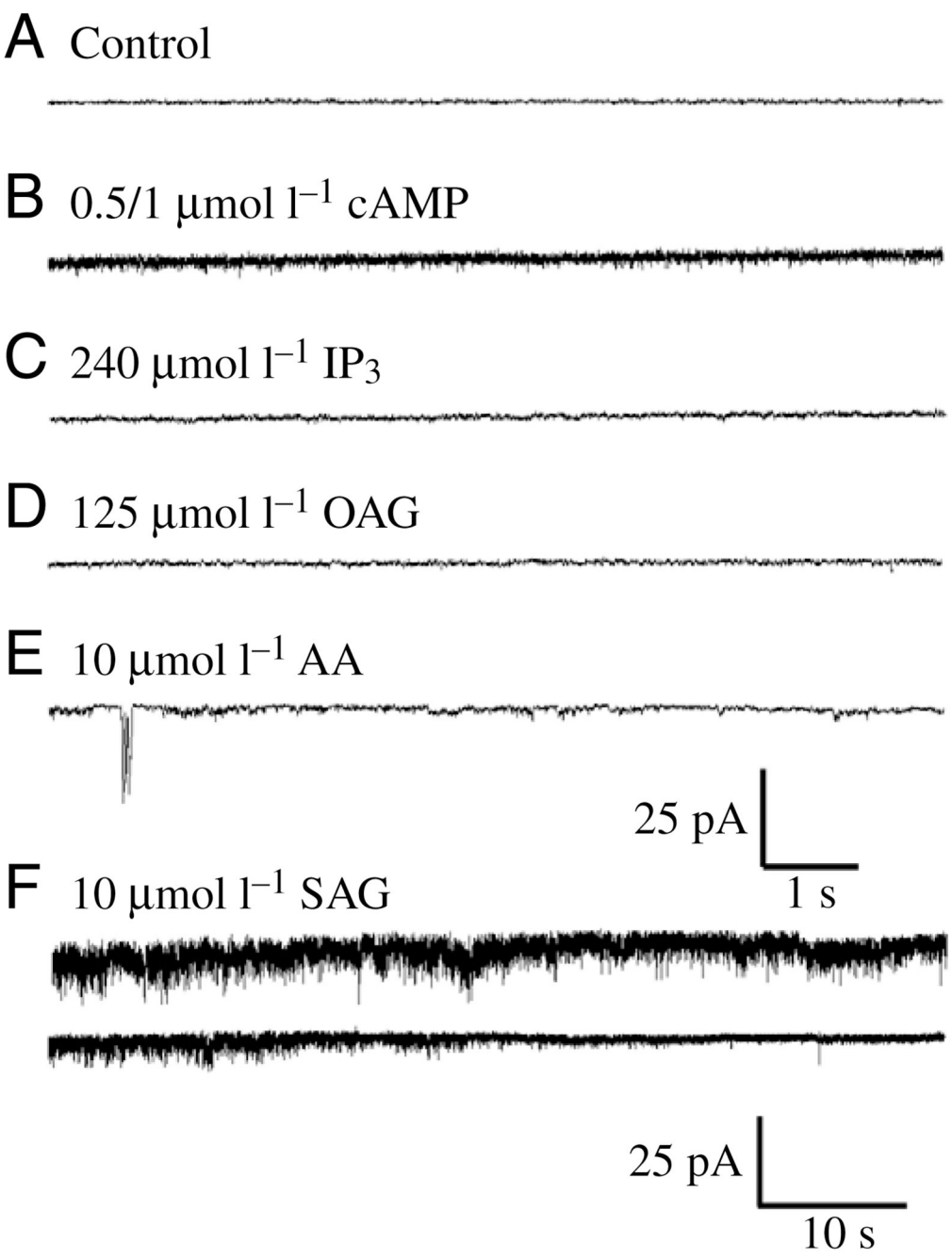

Fig. 5.

Dialysis of the second messengers cAMP, IP_3, OAG, arachidonic acid (AA), and SAG in isolated *S. odoratus* vomeronasal sensory neurons (VSNs). Analogues were made as described (see Materials and methods) and back-filled in the recording pipette to allow diffusion upon attaining the whole-cell configuration. VSNs were voltage-clamped at V_h=−60 mV. (A) A representative example of a VSN that had not been dialyzed with a second messenger analogue in order to illustrate stability of the patch. (B) 0.5 or 1 µmol l^{-1} cyclic adenosine monophosphate (cAMP) (*N*=27). (C) 240 µmol l^{-1} inositol 1,4,5-trisphosphate (IP_3) (*N*=20). (D) 125 µmol l^{-1} 1-oleoyl-2-acetyl-*sn*-glycerol (OAG), a membrane-permeant analogue of diacylglycerol (DAG), applied to either the bath surrounding the VSN or within the recording pipette (*N*=15).

Trace shown is an example of pipette perfusion. (E) 10 μmol l^{-1} AA, a polyunsaturated fatty acid (PUFA) derivative of DAG (*N*=11). (F) 10 mmol l^{-1} 1-stearoyl-2-arachidonoyl-*sn*-glycerol (SAG), a natural analogue of DAG (*N*=6).

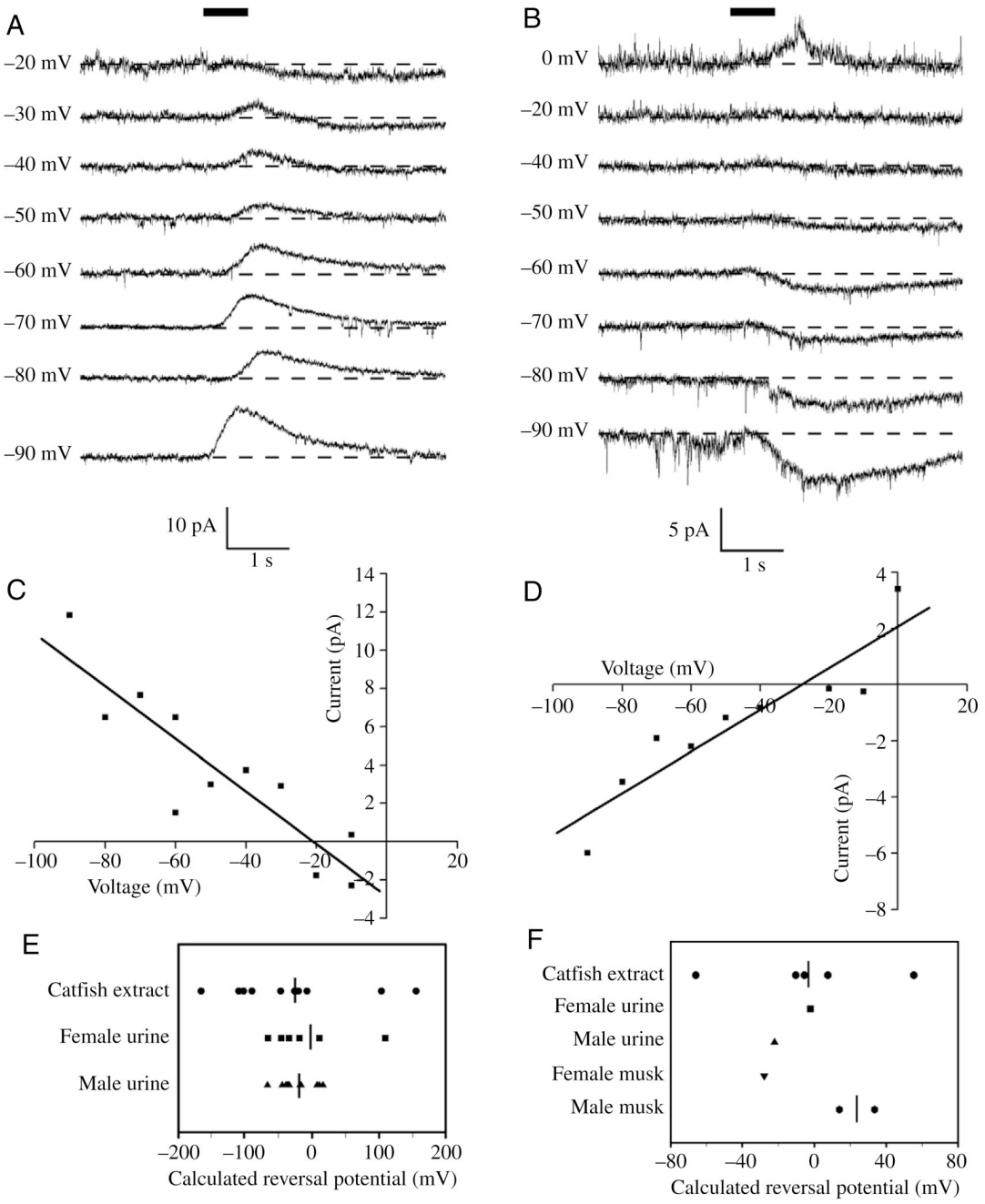

Fig. 6.

Analysis of chemosignal-activated reversal potentials supports a cationic receptor potential in vomeronasal sensory neurons (VSNs) of *S. odoratus*. (A,B) Response of a female neuron to (A) catfish extract (1:10 dilution), (B) female musk (1:100 dilution). Broken horizontal lines indicate baseline currents. (C,D) Plotted current–voltage relation for the families of currents evoked in A and B, respectively. (E,F) Scatter plot of estimated reversal potentials derived in C and D for chemosignal-evoked outward (E) and inward (F) currents, respectively. For each chemosignal, the vertical line depicts the mean reversal potential if more than one sample was obtained. The average reversal potential for the outward current was −28.2±2.37 mV (*N*=30) and that for the inward current was −5.7±7.79 mV (*N*=10).

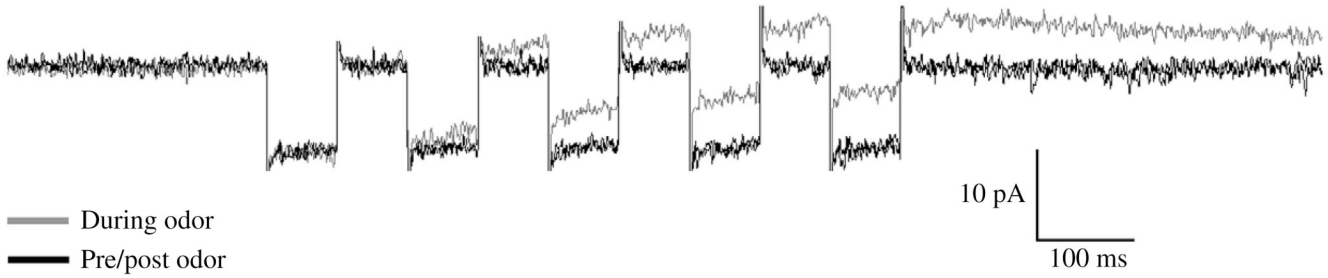

Fig. 7.

Vomeronasal sensory neurons (VSNs) from *S. odoratus* exhibit a chemosignal-evoked conductance decrease linked with outward currents. A VSN from a female *S. odoratus* was held at −60 mV (V_h) with five hyperpolarizing steps to −90 mV (V_c) injected prior (black), during (gray) and following (black) chemosignal stimulation with catfish extract. Inward chemosignal-evoked conductance changes were not tested.

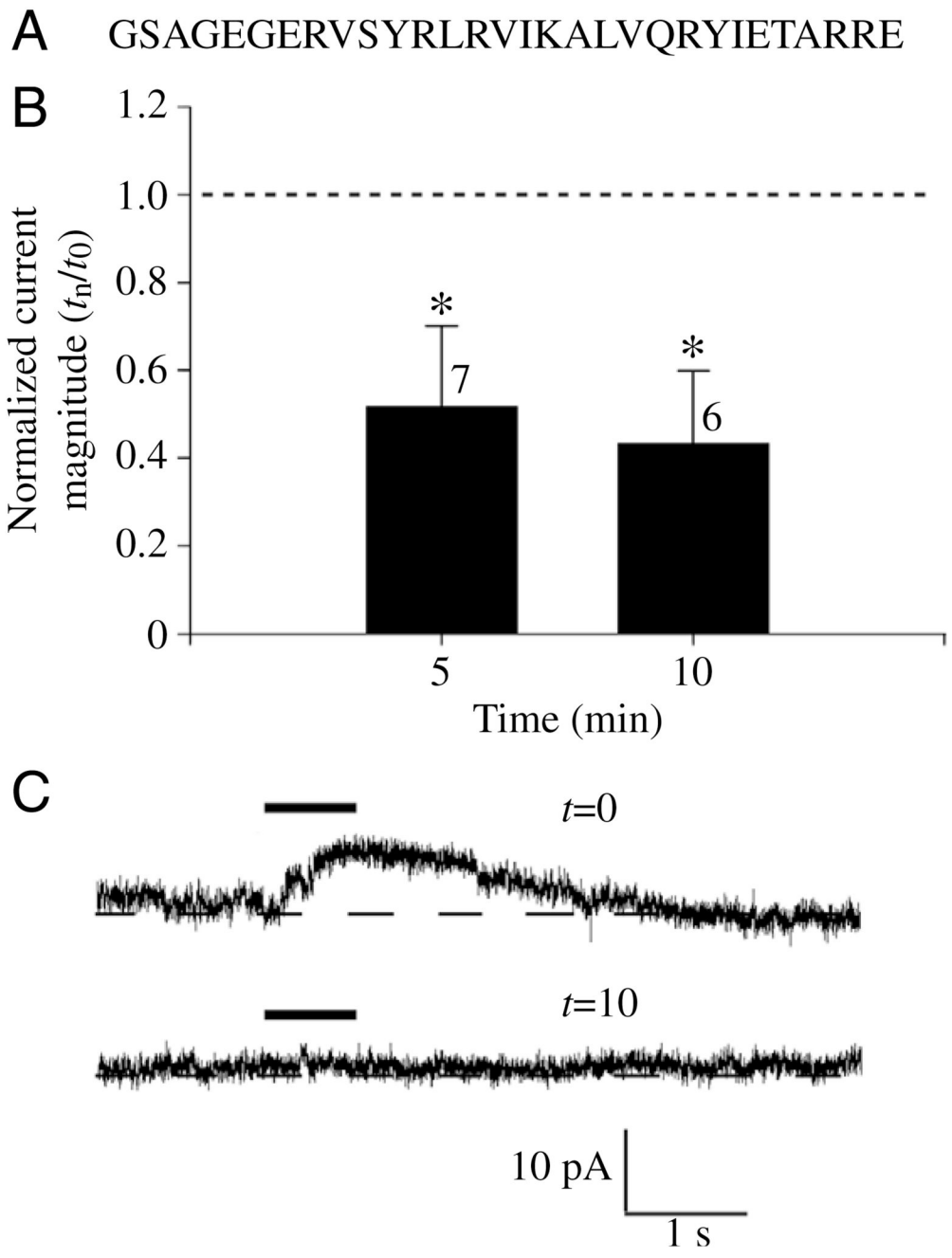

Fig. 8.

A peptide directed against the interaction domain between TRPC2 and IP_3R3 blocks the chemosignal-activated currents in *S. odoratus* vomeronasal sensory neurons (VSNs) when included in the patch pipette in the whole-cell configuration. (A) Amino acid sequence of the synthesized peptide (derived from mTRPC2, amino acids 905–934) (Tang et al., 2001). (B) Histogram plot of the chemosignal-activated current over 10 min when 10 μmol l^{-1} peptide is included in the recording pipette. The normal chemosignal-activated current over time is denoted by a broken line (see Fig. 4). Current obtained for each cell at varying time points (t_n) was normalized to its first exposure to chemosignal (t_0) Asterisks denote significant differences between control and peptide, two-way repeated measures ANOVA, followed by

SNK pairwise multiple comparison between treatment and time, $P \leq 0.05$). (C) Representative example of peptide treatment. While in the whole-cell configuration, the VSN was presented with a chemosignal, and a baseline (immediately after the whole-cell configuration was obtained) recording was made (top). The same chemosignal-activated current is shown 10 min after peptide infusion (bottom). Broken line denotes baseline current.